JCI insight

RESEARCH ARTICLE

Vaccine induction of antibodies and tissue-resident CD8+ T cells enhances protection against mucosal SHIV-infection in young macaques

Caroline Petitdemange,[1] Sudhir Pai Kasturi,[1] Pamela A. Kozlowski,[2] Rafiq Nabi,[2] Clare F. Quarnstrom,[3] Pradeep Babu Jagadeesh Reddy,[1] Cynthia A. Derdeyn,[4] Lori M. Spicer,[4] Parin Patel,[1] Traci Legere,[1] Yevgeniy O. Kovalenkov,[5] Celia C. Labranche,[6] François Villinger,[7] Mark Tomai,[8] John Vasilakos,[8] Barton Haynes,[6] C. Yong Kang,[9] James S. Gibbs,[10] Jonathan W. Yewdell,[10] Dan Barouch,[11] Jens Wrammert,[5] David Montefiori,[6] Eric Hunter,[1] Rama R. Amara,[1] David Masopust,[3] and Bali Pulendran[12]

[1]Emory Vaccine Center, Yerkes National Primate Research Center at Emory University, Atlanta, Georgia, USA. [2]Department of Microbiology, Immunology, and Parasitology, Louisiana State University Health Sciences Center, New Orleans, Louisiana, USA. [3]Department of Microbiology and Immunology, Center for Immunology, University of Minnesota, Minneapolis, Minnesota, USA. [4]Department of Pathology and Laboratory Medicine, Emory Vaccine Center, and Yerkes National Primate Research Center. [5]Emory Vaccine Center, School of Medicine, Emory University, Atlanta, Georgia, USA. [6]Duke Human Vaccine Institute, Duke University School of Medicine, Durham, North Carolina, USA. [7]New Iberia Research Center, University of Louisiana Lafayette, Lafayette, Louisiana, USA. [8]3M Drug Delivery Systems, Saint Paul, Minnesota, USA. [9]Schulich School of Medicine & Dentistry, The University of Western Ontario, London, Ontario, Canada. [10]Cellular Biology Section, Laboratory of Viral Diseases, NIAID, NIH, Bethesda, Maryland, USA. [11]Center for Virology and Vaccine Research, Beth Israel Deaconess Medical Center, Harvard Medical School, Boston, Massachusetts, USA. [12]Departments of Pathology, and Microbiology & Immunology, Institute for Immunity, Transplantation and Infection, Stanford University, Stanford, California, USA.

Antibodies and cytotoxic T cells represent 2 arms of host defense against pathogens. We hypothesized that vaccines that induce both high-magnitude CD8+ T cell responses and antibody responses might confer enhanced protection against HIV. To test this hypothesis, we immunized 3 groups of nonhuman primates: (a) Group 1, which includes sequential immunization regimen involving heterologous viral vectors (HVVs) comprising vesicular stomatitis virus, vaccinia virus, and adenovirus serotype 5–expressing SIVmac239 Gag; (b) Group 2, which includes immunization with a clade C HIV-1 envelope (Env) gp140 protein adjuvanted with nanoparticles containing a TLR7/8 agonist (3M-052); and (c) Group 3, which includes a combination of both regimens. Immunization with HVVs induced very high–magnitude Gag-specific CD8+ T cell responses in blood and tissue-resident CD8+ memory T cells in vaginal mucosa. Immunization with 3M-052 adjuvanted Env protein induced robust and persistent antibody responses and long-lasting innate responses. Despite similar antibody titers in Groups 2 and 3, there was enhanced protection in the younger animals in Group 3, against intravaginal infection with a heterologous SHIV strain. This protection correlated with the magnitude of the serum and vaginal Env-specific antibody titers on the day of challenge. Thus, vaccination strategies that induce both CD8+ T cell and antibody responses can confer enhanced protection against infection.

Authorship note: CP and SPK contributed equally to this work.

Conflict of interest: The authors have declared that no conflict of interests exists.

Submitted: November 8, 2018
Accepted: January 11, 2019
Published: February 21, 2019

Reference information:
JCI Insight. 2019;4(4):e126047.
https://doi.org/10.1172/jci.insight.126047.

Introduction

Thirty years ago, HIV-1 was identified as the causative agent of AIDS. Despite seminal advances in the development of therapeutics to control HIV infection, and great progress in understanding the pathogenesis of HIV and the immunological mechanisms that mediate protection, the development of an effective vaccine remains elusive. Although much recent effort has focused on understanding the critical roles played by neutralizing antibodies in conferring protection against HIV (1, 2), the full spectrum of immunological

mechanisms and the extent to which they might synergize to mediate protection is poorly understood. To date, the RV144 clinical trial, in which a vaccination regimen involving a canarypox viral vector prime (ALVAC-HIV) and an envelope gp120 protein boost (AIDSVAX B/E) was assessed, remains the only vaccine trial against HIV to our knowledge that has shown even a modest degree of efficacy, affording only partial protection with a 31.2% reduction in HIV acquisition after 42 months (3). Retrospective, case-controlled analysis to identify immune correlates of infection risk revealed that binding of IgG antibodies to variable regions 1 and 2 (V1V2) of HIV-1 envelope proteins (Env) correlated inversely with the rate of HIV-1 infection (4).

A major limitation of the ALVAC/AIDSVAX regimen was the short durability of protection (3). Indeed, induction of durable antibody responses has posed a challenge in HIV vaccine development and for vaccinology in general. It is now clear that the innate immune system plays a fundamental role in programming the magnitude, quality, and durability of the adaptive immune response (5, 6). Our previous work has demonstrated that the live attenuated yellow fever vaccine YF-17D induces robust $CD8^+$ T cell responses and antibody responses, via activation of TLR on DC subsets (7, 8). Furthermore, recent work in our laboratory determined in a mouse model that delivery of a specific combination of TLR ligands encapsulated in nanoparticles (NP) with antigens, induced enhanced DC activation, and increased antigen-specific T cells, long-lived antibody responses, persistent germinal centers, and lymph node–resident plasma cells up to 1.5 years (9).

The potential of NP-encapsulated TLR ligands as a vaccine adjuvant has been confirmed in a nonhuman primate (NHP) study where we observed that NP-encapsulated TLR4 and TLR7/8 (MPL + R848) agonists administered with a soluble Env protein promoted robust and durable antibody responses in serum and mucosal secretions that correlated with enhanced protection against SIVsmE660 mucosal challenge (10).

Generating large numbers of antiviral cytotoxic $CD8^+$ T cells has been another goal in HIV vaccine development. $CD8^+$ T cells are thought to confer protection against HIV (11–13), but induction of high magnitude $CD8^+$ T cell responses, especially in the mucosal tissue, has been a challenge. Viral vectors such as yellow fever (7, 14) and vaccinia virus (15) induce strong $CD8^+$ T cell responses in humans. Recently, we have shown in mice that the heterologous viral vector (HVV) vaccination regimen consisting of sequential immunization with vesicular stomatitis virus (VSV) and vaccinia virus (VV) vectors expressing the same antigen resulted in robust antigen-specific $CD8^+$ T cell responses and the generation of tissue-resident memory (TRM) $CD8^+$ T cells, which retained effector-like properties and accumulated preferentially in nonlymphoid tissues (16–18). Such a strategy to induce high frequencies of $CD8^+$ T cells in mucosal tissues at the portals of HIV entry, in concert with an Env immunogen that induces robust antibody responses, could offer a multipronged approach to prevent HIV infection.

In this trial, we investigated the hypothesis that a multicomponent vaccine approach that stimulates a strong and persistent Env-specific antibody response (using the potentially novel TLR7/8 agonist 3M imidazoquinoline molecule 3M-052), along with Gag-expressing HVV to stimulate a Gag-specific $CD8^+$ T cell response, might enhance protection against mucosal simian/human immunodeficiency virus (SHIV) challenge. The adjuvant 3M-052 is designed for a slow dissemination from the site of application (19) and has been shown to enhance antibody and Th1-type cellular immune responses to HIV vaccine antigens (20). In order to test the efficacy of each component independently, we evaluated 3 groups of rhesus macaques (RMs) vaccinated as follows: (a) HVV alone, (b) NP encapsulated 3M-052 adjuvanted gp140 Env protein (Env + NP), or (c) a sequential vaccination regimen involving HVV and Env + NP. Immunization with HVV induced robust Gag-specific $CD8^+$ T cells and a very high frequency of tissue-resident $CD8^+$ T cells. Immunization with Env + NP induced robust and persistent Env-specific antibody responses and BM plasma cell responses. Immunization with the HVV regimen and Env + NP induced both Gag-specific $CD8^+$ T cells and tissue-resident $CD8^+$ T cells, as well as robust antibody and persistent plasma cell responses. Since the age distribution of the animals in the study was wide (3–16 years), we divided the groups into younger (<8 years) and older (>8 years) animals, based on the fact that RMs do not reach adult body size until about 8 years of age (21). Interestingly, after 10 weekly intravaginal challenges with the heterologous pathogenic CCR5-tropic subtype C SHIV-1157ipd3N4 virus strain (considered to represent a stringent NHP challenge mode; ref. 22), significant protection was observed in young animals (<8 years old) in the HVV + NP group, relative to that observed in young animals in the HVV- or NP-alone groups. Serum and vaginal binding antibodies specific for the Env immunogen, antibody-dependent cell-mediated virus inhibition (ADCVI) of the challenge virus, and neutralizing antibodies to Tier 1 virus strains were directly correlated with protection in HVV, Env + NP–vaccinated animals.

Results

Vaccination with HVV + NP induces enhanced protection against a low-dose, heterologous, intravaginal SHIV challenge. We evaluated whether stimulation of both humoral and cellular immune responses through a sequential immunization strategy with a series of Gag-expressing viral vectors (VSV, VV, and adenovirus serotype 5 [Ad5]), followed by Env protein adjuvanted with the TLR7/8 agonist 3M-052 encapsulated in polylactic glycolic acid (PLGA) NP, could enhance protection in a repeated low-dose SHIV intravaginal challenge model. Thus, 66 female RMs (Supplemental Table 1; supplemental material available online with this article; https://doi.org/10.1172/jci.insight.126047DS1) were assigned to 1 of 3 immunization groups (Figure 1A). The 23 animals in Group 1 were immunized only with HVV encoding full-length SIVmac239 Gag protein as follows: VSV at week 0, VV at week 9, and Ad5 at week 37. The animals in Group 2 were immunized 4 times at weeks 15, 21, 29, and 39, with a recombinant Clade C HIV Env protein (gp140 C.1086 K160N) adjuvanted with 3M-052 encapsulated in NP, as performed in our previous study where this immunization modality was shown to efficiently induce high and persistent Env-IgG responses (10). Finally, the 21 animals in Group 3 were immunized sequentially with both HVV and NP adjuvanted Env protein (Figure 1B). We compared immunogenicity and efficacy of the 3 vaccine regimens relative to 15 unvaccinated control animals. One month (week 54) before challenges were initiated, 4 animals in each vaccine group were necropsied for tissue analysis. Four months after the final immunization, all remaining RMs were challenged once weekly by the intravaginal route with SHIV-1157ipd3N4 until infection (plasma viral load ≥ 60 copies of viral RNA/ml for 2 consecutive weeks) or for a total of 10 challenges. Although we did not observe any long-term protection after 10 challenges in any of the groups, we observed a near-significant protection after 5 challenges for animals vaccinated with Env + NP component (Gehan-Breslow test; $P = 0.0541$ and $P = 0.0530$ for Env + NP and HVV, Env + NP groups, respectively) (Figure 1C). Interestingly, 80% of younger animals (<8 years) vaccinated with the combination of HVV and Env + NP regimen were protected after 5 challenges and exhibited significantly higher protection than older animals up to the tenth challenge (Gehan-Breslow test $P = 0.0278$, Log-rank test, $P = 0.0337$). Furthermore, both the HVV-alone or Env + NP–alone vaccinated groups showed significant protection until the fifth challenge (Gehan-Breslow test, $P = 0.0082$ and $P = 0.0398$ for HVV and Env + NP groups, respectively), but protection was not apparent after the tenth challenge (Figure 1D). The presence of Mamu-A*01 or TRIM5α alleles were not associated with better protection in animals vaccinated with HVV or HVV, Env + NP immunizations (data not shown). Furthermore, animals immunized with HVV displayed significantly reduced peak plasma viremia when compared with naive controls, suggesting a role for T cell responses in the early control of viral infection, once established (Supplemental Figure 1A). Vaccination also had a significant impact on viral control at 3 weeks after infection for HVV and HVV, Env + NP, and at 5 weeks after infection for HVV-vaccinated animals (Supplemental Figure 1B).

High-magnitude and persistent Gag-specific CD4$^+$ and CD8$^+$ T cell responses after immunization with HVV. We evaluated the frequencies of p11c CM9 Gag–specific CD8$^+$ T cells by tetramer staining in blood of Mamu-A*01$^+$ RMs. After the Ad5 immunization, we observed remarkably high responses, with as much as 65% of the total CD8$^+$ T cells being CM9 tetramer$^+$ cells at 1 week after the Ad5 vaccination; this elevated frequency was maintained for several weeks (mean, 37.6% at week 38) (Figure 2, A and B). Frequencies of SIV Gag–specific CD4$^+$ and CD8$^+$ T cells producing IFN-γ, TNF-α, and IL-2 were assessed by intracellular cytokine staining (ICS) after stimulation with a SIV Gag peptide pools following VSV, VV, and Ad5 immunizations. There was a substantial Gag-specific CD4$^+$ T cell response after VSV immunization, which increased after VV and Ad5 immunizations (Figure 2C). In the case of CD8$^+$ T cells, the responses measured 1 week after VSV immunization were significantly boosted by VV and Ad5 vaccinations, with remarkably high magnitudes of CD8$^+$ T cell responses (up to 20% IFN-γ–producing cells at week 38; mean, 6.6%) (Figure 2D). Polyfunctional T cells capable of simultaneously secreting IFN-γ, TNF-α, and IL-2 were detected after VV immunization, and these were expanded by Ad5 boosting (Supplemental Figure 2). However, the dominant T cell populations were those that produced IFN-γ alone or both IFN-γ and TNF-α (Supplemental Figure 2). T cell responses induced by HVV were persistent at memory time points, and we observed comparable responses in HVV and HVV, Env + NP treatment groups, suggesting that Env + NP immunizations did not impact the magnitude of CD4$^+$ and CD8$^+$ T cell responses (Figure 2, B–D). We also assessed the Env-specific CD4$^+$ and CD8$^+$ T cell responses. CD4$^+$ T cell responses peaked at 1 week after each Env + NP immunization, but CD8$^+$ T cell responses were negligible (Figure 2, E and F). Env-specific CD4$^+$ T cell responses induced by the Env + NP and HVV, Env + NP vaccination regimens were similar,

A

Groups of vaccination	Numbers of animals (n) Immunization	Necropsy	Challenge	Immunogens	Dose
Gr 1 Heterologous Viral vectors (HVV)	23	4	19	HVV expressing p55 Gag protein: Vesicular stomatitis virus (VSV) Vaccinia virus (VV) Adenovirus serotype 5 (Ad5)	$5x10^7$ pfu $1x10^7$ pfu $7x10^{10}$ pfu
Gr 2 Envelope + NP (Env + NP)	22	4	18	C.1086 K160N Env gp140 trimer protein + TLR7/8 agonist (3M052) encapsulated in PLGA Nanoparticles (NP)	100 μg 75 μg 2 mg
Gr 3 HVV, Env + NP	20	4	16	VSV + VV + Ad5 + Env gp140 + TLR7/8 NP	

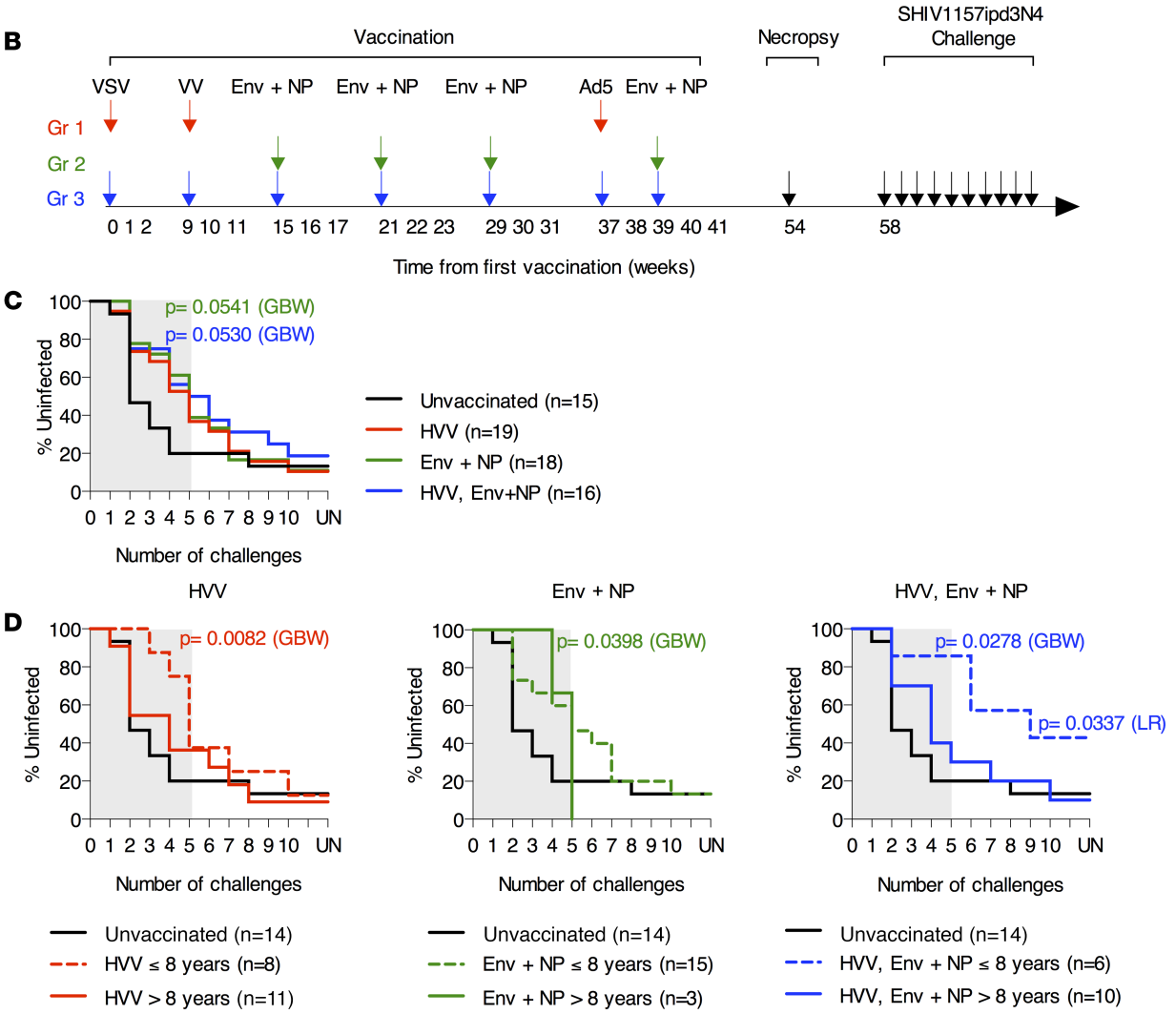

Figure 1. Vaccination that induces both antibody and tissue-resident CD8⁺ T cell responses confer enhanced protection against mucosal SHIV infection in young macaques. (**A**) Vaccination groups and immunogens: 65 female RMs of ages 5–15 years were divided into 3 experimental groups. Animals in Group 1 were sequentially immunized with replication competent recombinant heterologous viral vectors (HVV) VSV, VV, and Ad5 each encoding SIVmac239 Gag protein. Animals in Group 2 were immunized with recombinant gp140 C.1086 K160N trimeric Env protein adjuvanted with the TLR7/8 agonist, 3M-052, encapsulated in PLGA nanoparticles (NP). Group 3 animals received immunizations with both HVV and adjuvanted Env protein, according to schedule indicated. (**B**) Study overview. Animals were bled 4 weeks before primary immunization for baseline analysis. Immunization was performed with each viral vector or adjuvanted Env protein on the weeks indicated by arrows. At week 54, 4 animals in each group were sacrificed to evaluate prechallenge immune responses. Starting at week 58, the remaining animals were challenged weekly by the intravaginal route a total of 10 times or until infected with SHIV-1157ipd3N4, which expresses a heterologous Clade C Env. (**C**) Rate of infection acquisition in all vaccinated animals in comparison with the 15 unvaccinated controls. The gray section highlights SHIV acquisition up to 5 challenges. (**D**) Acquisition of infection in animals <8 years old (dotted line) and animals >8 years old (solid line). When compared with young unvaccinated controls, younger animals (<8 years) given the HVV, Env + NP vaccine regimen were found to be significantly protected using the Mantel-Cox Log-rank test or Gehan-Breslow Wilcoxon test for early time points.

except at week 40, after the last protein boost, where we observed a significantly higher response in HVV, Env + NP–vaccinated animals (Figure 2E).

Immunization with NP adjuvanted Env protein induced robust and durable antibody responses. We measured antibody responses induced in animals vaccinated with the Env + NP or HVV, Env + NP regimens. Gp140 C.1086 K160N–specific IgG binding antibodies in serum were measured by ELISA, at baseline and at 2 weeks after immunizations. IgG responses were significantly boosted in both HVV, Env + NP, and Env + NP vaccination groups 2 weeks after the second immunization (week 23), with an increase of 218-fold (Env + NP) and 137-fold (HVV, Env + NP) in comparison with the peak after the first immunization (week 17) (Figure 3A).

The highest responses were measured 2 weeks after the third gp140 immunization (week 31) in the Env + NP group, with a mean concentration of 2410 μg/ml, and after the fourth gp140 immunization in the HVV, Env + NP group, with a mean of 2128 μg/ml. IgG antibody levels then declined to 617 μg/ml (Env + NP) and 443 μg/ml (HVV, Env + NP) by week 58 (the day of challenge), with no significant differences observed between the groups (Figure 3A). We also detected Env-specific IgG binding antibody responses in vaginal secretions at week 54, with a similar level of antibodies in both groups of vaccination (Figure 3B).

High avidity anti-Env serum IgG antibodies in vaccinated NHP have been associated with reduced acquisition (23) of infection and viral load following SHIV or SIV challenge exposure (24). We measured the avidity of antibodies specific for gp140 C.1086 K160N and gp120 1157ipd3N4 Env proteins on the day of challenge (week 58), and we observed higher avidities in HVV, Env + NP–vaccinated animals (median avidity index, 37.9 for gp140 C.1086 and 13.0 for gp120 1157ipd3N4) in comparison with Env + NP–vaccinated animals (median avidity index, 26.7 for C.1086 gp140 and 6.5 for gp120 1157ipd3N4) (Figure 3, C and D). We also analyzed neutralization titers 2 weeks after the last protein boost (week 41) and observed high titers of neutralizing antibodies against the MW965.26 Tier 1A virus (median HVV, Env + NP = 23,056; median Env + NP = 32,060) and the 6644.v2.c33 Tier 1B virus (median HVV, Env + NP = 370; median Env + NP = 458.3). Titers of Tier 1A and Tier 1B neutralizing antibodies decreased by ~5-fold at week 54 but were maintained at this level until the day of challenge. However, the vaccine was not effective in inducing neutralizing antibodies against the Tier 2 SHIV-1157ipd3N4 challenge virus (Figure 3D).

In addition, we measured ADCVI activity, which is triggered when an antibody bound to antigen expressed on virus-infected cells engages the Fcγ receptor (FcγR) on effector cells, such as NK cells, monocytes, or macrophages. This can lead to lysis of the virus-infected target cells (antibody-dependent cellular cytotoxicity [ADCC]) or to noncytolytic mechanisms or viral inhibition, such as β-chemokine release from the effector cells. ADCVI antibody activity has been associated with protection from SHIV infections in macaques (25, 26). Thus, we also measured ADCVI activity in serum on the day of challenge using SHIV-1157ipd3N4-infected target cells. Similar inhibition of viral infection was observed in the Env + NP and HVV, Env + NP groups (Figure 3E). Various studies have described age-related changes in the magnitude of antibody responses in humans and macaques (27–29). Indeed, comparisons of anti-Env antibody responses in young and adolescent (<8 years old) with older (>8 years old) HVV, Env + NP–vaccinated animals revealed significant differences (Supplemental Figure 3). We observed significantly higher concentrations of gp140-specific serum IgG and vaginal IgG in younger animals (Supplemental Figure 3, A and B). Conversely, older animals displayed significantly higher anti-gp140 serum IgM concentrations (Supplemental Figure 3C).

Robust induction of Env-specific plasmablasts and long-lived plasma cells in BM by 3M-052 adjuvanted Env immunizations. Following vaccination, activated B cells can differentiate into antibody-secreting plasma cells in the draining lymph nodes or can migrate into B cell follicles, where they divide rapidly to form germinal centers (30, 31). Germinal centers are the microenvironments where B cells can differentiate into memory B cells or long-lived plasma cells that traffic to the BM (30, 31). Recall vaccination in humans (32) or macaques (10) is characterized by a striking increase in antibody-secreting plasmablasts within 7 or 4 days, respectively, of vaccination. Consistent with this, we observed that IgG and IgA gp140–specific plasmablast responses in blood were strikingly higher on day 4 after recall vaccination, with more modest effects observed at day 7 (Figure 4, A and B). With the exception of day 7 following the second protein immunization, Env + NP– and HVV, Env + NP–vaccinated animals exhibited comparable increases in anti-gp140 IgG and IgA plasmablasts (Figure 4, A and B) and very few IgM secreting cells (Supplemental Figure 4A). There were also substantial numbers of gp140-specific IgG and IgA, but negligible IgM plasma cells in the BM at weeks 44 and 49 (Figure 4, C and D, and Supplemental Figure 4B), although there were no significant differences between vaccination groups.

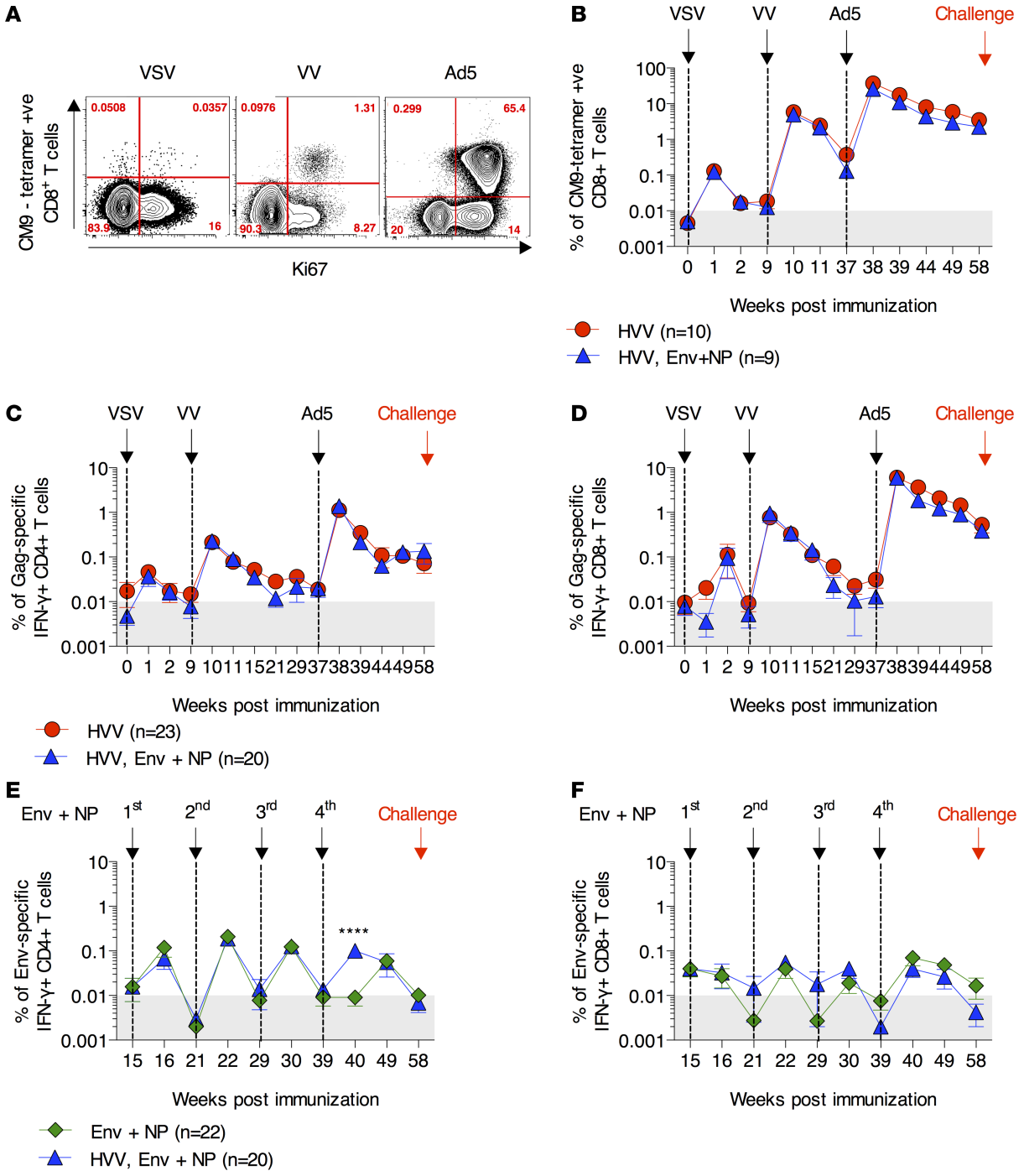

Figure 2. High magnitude and persistent SIV Gag-specific CD4⁺ and CD8⁺ T cell responses induced by immunization with heterologous viral vectors. (**A**) Flow cytometry dot plots illustrating expansion of CM9 tetramer⁺CD8⁺ T cells after VSV-, VV-, and Ad5-SIV Gag immunizations. (**B**) Kinetics of CM9 tetramer⁺CD8⁺ T cell responses in Mamu-A*01⁺ animals immunized with HVV alone (red) or with HVV, Env + NP (blue). (**C** and **D**) Kinetics of SIV Gag–specific IFN-γ–producing CD4⁺ and CD8⁺ T cells measured by ICS after stimulation of PBMC with SIVmac239 Gag peptides. (**E** and **F**) Kinetics of HIV Env–specific CD4⁺ and CD8⁺ T cells producing IFN-γ measured by ICS after stimulation of PBMC with an Env peptide pool. Gray lines represent the threshold cut-off value (0.01) after background subtraction. In all graphs, geometric mean values and ± SD are presented. Asterisks denote significant differences between groups. ****$P \leq 0.0001$ by 2-tailed Mann-Whitney rank sum test.

Robust and sustained activation of monocytes and DCs after immunization with Env protein and 3M-052. The innate immune response plays a fundamental role in modulating the magnitude and durability of antibody responses. Therefore, in order to gain insights into the mechanisms by which 3M-052 might induce such robust and durable antibody responses, we analyzed the early innate responses stimulated

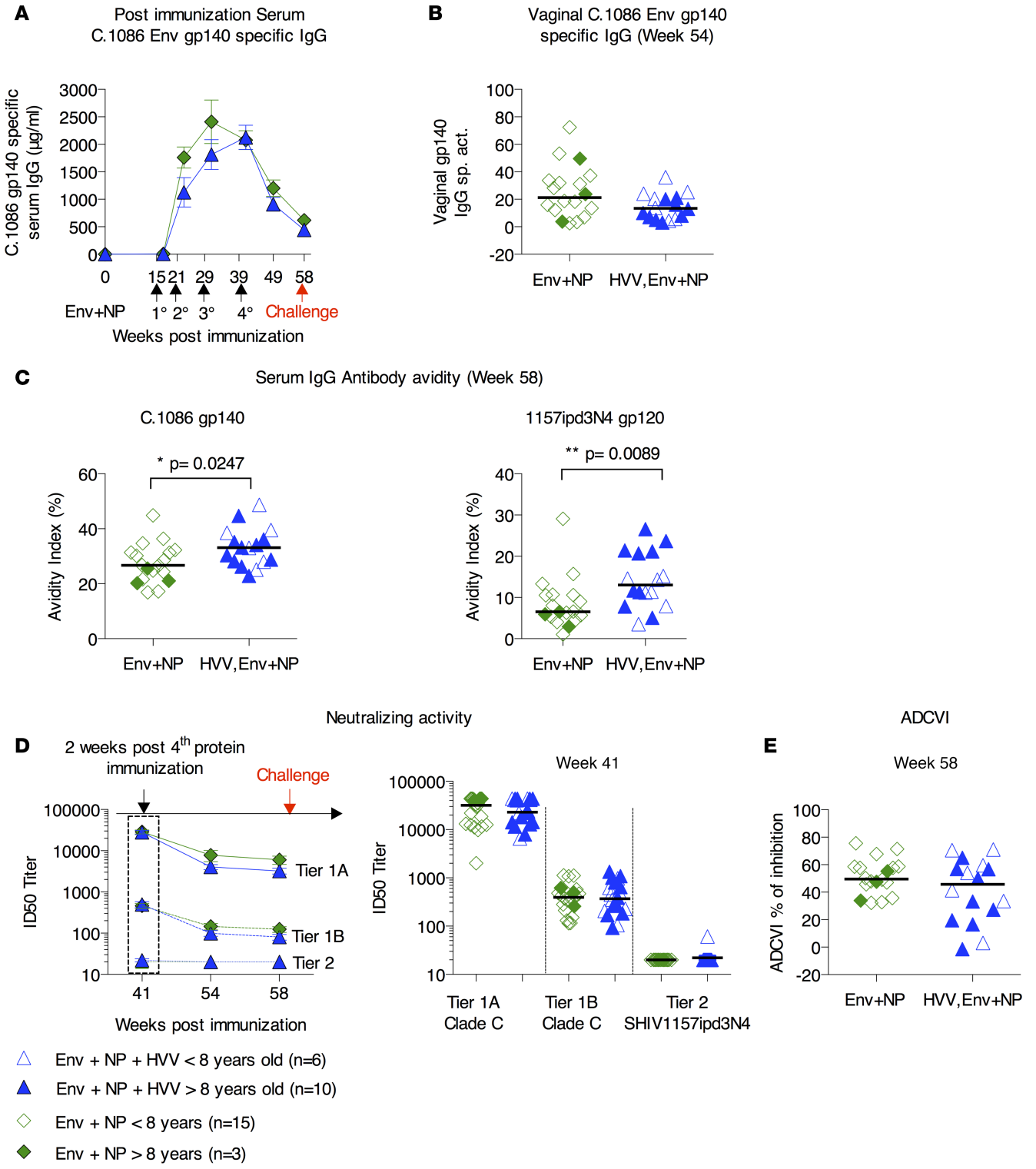

Figure 3. High magnitude and persistent antibody responses induced by immunization with Env protein and TLR7/8 ligand containing PLGA nanoparticles. (**A**) Concentrations of gp140 C.1086 K160N–specific IgG binding antibodies were measured by ELISA in serum 2 weeks after the first, second, third, and fourth Env protein immunization in animals vaccinated with Env + NP alone (green) or HVV, Env + NP (blue). Geometric mean values and ± SD are shown. (**B**) Levels of C. 1086 K160N gp140–specific vaginal IgG antibodies in 1 month before challenge (week 54). Bars represent medians. (**C**) Avidity indices of serum IgG antibodies specific for the gp140 C.1086 K160N immunogen or gp120 1157ipd3N4 protein measured at week 58 (day of challenge). Bars represent medians. (**D**) Titers of neutralizing antibodies measured against MW965.26 Tier 1A virus (solid line), 6644.v2.c33 Tier 1B virus (dotted line), and the SHIV-1157ipd3N4 Tier 2 challenge virus (thin dotted line). (**E**) ADCVI activity measured in serum on the day of challenge. Bars represent medians. Significance differences between groups were determined using the 2-tailed Mann-Whitney test. Open triangles and diamonds represent animals younger than 8 years old; closed triangles and diamonds represent animals > 8 years.

by vaccination with 3M-052 adjuvanted Env. In particular, we analyzed the changes in the frequency and activation status of monocytes and myeloid and plasmacytoid DCs (mDCs and pDCs, respectively) in peripheral blood mononuclear cells (PBMCs). We first evaluated the frequencies of the different monocyte subsets, (classical $CD14^+CD16^-$, intermediate $CD14^+CD16^+$, and nonclassical $CD14^-CD16^+$ monocytes) (Supplemental Figure 5). Vaccination with any of the viral vectors or with Env + NP induced a significant expansion of intermediate $CD14^+CD16^+$ monocytes with the greatest ~4-fold (VSV) and ~8-fold (Env + NP) increases at day 1 in comparison with day 0 (Supplemental Figure 5B). In contrast, VV and Ad5 immunizations induced only a modest expansion (~2-fold increase) (Supplemental Figure 5B). Increases of inflammatory monocytes coincided with the diminution of classical $CD14^+CD16$– monocytes on day 1 and day 2 (Supplemental Figure 5B). Little effect on nonclassical monocytes was seen with any of the immunization stimuli. Intermediate and classical monocytes were highly activated after vaccination, as evidenced by enhanced expression of CD86 and CCR7 (Figure 5, A and B). CD86 and CCR7 upregulation peaked at day 1 and day 2 following VSV, VV, and Ad5 immunizations. Remarkably, following Env + NP immunization, we observed enhanced and sustained innate activation that was maintained until at least 2 weeks after immunization. We did not observe significant differences between immunization groups for CCR7 expression by classical and intermediate monocytes, except at day 1 after Ad5 immunization (Figure 5B).

We next analyzed the dynamics of activation of pDC, as well as BDCA-1^+ and $CD11c^+$ mDC subsets. Vaccination with VSV and Ad5 viral vectors markedly increased pDC frequencies on day 1 and returned to baseline levels on day 4 (Supplemental Figure 6). All immunizations enhanced expression of CCR7 and CD86 activation markers on pDCs (Supplemental Figure 7). BDCA-1^+ mDC frequencies were increased after VSV (day 1) and Env + NP (day 1, 4 and 14) immunizations, while VV and Ad5 induced a diminution of this population. By contrast, VV and Ad5 promoted a significant expansion of $CD11c^+$ mDCs on day 4 and day 7. Once again, upregulation and sustained expression of CD86 and CCR7 activation markers were mainly observed after Env + NP vaccination (Supplemental Figure 7). Overall, we observed a significant and early activation of monocytes and DCs, especially between day 1 and day 4 after vaccination, with recruitment of distinct subpopulations according to the type of vaccination.

Correlation of prechallenge antibody responses with rate of acquisition in HVV, Env + NP–vaccinated animals. Given the significant protection against infection provided by vaccination (Figure 1D), we sought to define correlates of protection. Comparison of prechallenge Env–specific serum binding antibodies with the number of challenges required for infection revealed a direct correlation between the number of challenges required for infection and the concentration of gp140 C.1086 K160N–specific IgG, gp41-specific IgG, and anti–C1 IgG antibodies in the serum (Figure 6, A–C). Importantly, the concentration of gp140-specific vaginal IgG antibodies was also correlated with the number of challenges required for infection (Figure 6D). In addition to binding antibodies, BM plasma cells measured at week 44 and serum ADCVI activity correlated with the number of challenges required for infection in HVV, Env + NP–vaccinated animals (Figure 6, E and F). Finally, titers of Tier 1A MW965.26 and Tier 1 SHIV-1157ipEL-p neutralizing antibodies were also correlated with the number of challenges needed for infection (Figure 6G). Interestingly, these antibody responses did not correlate with rate of acquisition in animals vaccinated with Env + NP only (Supplemental Figure 8).

HVV induce SIV-specific memory $CD8^+$ T cells within tissues. We aimed to determine the establishment and distribution of the vaccine-elicited Gag- specific memory $CD8^+$ T population. Seventeen weeks after the final vector vaccination and 1 month prior to the vaginal challenge, we necropsied 2 animals in the HVV and HVV, Env + NP immunization groups. We measured CM9 tetramer cells in the blood, iliac lymph node, vagina, and cervix. By flow cytometry, we observed abundant Gag-specific memory $CD8^+$ T cells in blood and iliac lymph node but, importantly, also in the vaginal and cervical mucosa, which represent the site of viral challenge and portal of viral entry (Figure 7A). To quantify Gag-specific memory $CD8^+$ T cells in the mucosa, we stained tissue sections with CM9 tetramers and enumerated $tetramer^+$ cells relative to total $DAPI^+$ nucleated cells (Figure 7, B and C). Representative staining in the vaginal mucosa highlighted the presence of $tetramer^+$memory $CD8^+$ T cells subjacent to the vaginal epithelium and in close proximity to $CD4^+$ T cells (Figure 7C). To test function, lymphocytes were isolated from the indicated tissues and stimulated with CM9 peptide overnight (Figure 7D). Subsequent analysis revealed that vaccine-elicited Gag CM9–specific memory $CD8^+$ T cells underwent degranulation in response to peptide stimulation, suggesting that they were capable of killing virus-infected target cells. Moreover, IFN-γ was expressed (Figure 7D), which has been associated with the ability of TRM to induce an antiviral response and to recruit B cells to the reproductive mucosa (33, 34).

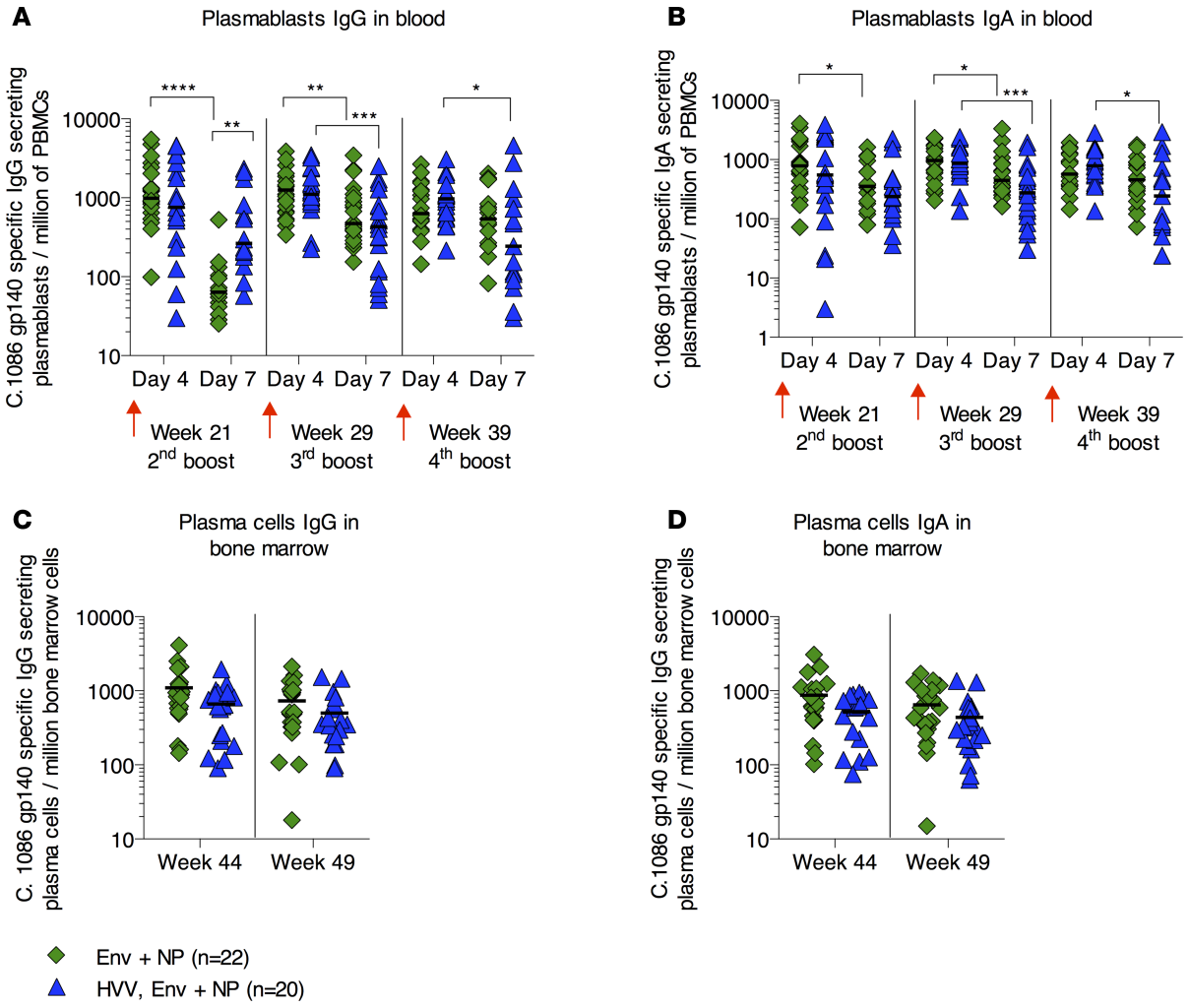

Figure 4. Induction of Env-specific plasmablasts in blood and long-lived plasma cells in BM by adjuvanted Env protein immunizations. (**A** and **B**) C.1086 K160N gp140–specific IgG and IgA plasmablasts measured by ELISPOT in blood collected on day 4 and day 7 after the 2nd (week 21), 3rd (week 29), and 4th (week 39) Env protein immunization in animals vaccinated with Env + NP (green) or HVV, Env + NP (blue). Bars represent medians. (**C** and **D**) Gp140 C.1086 K160N–specific IgG and IgA plasma cells measured 5 weeks (week 44) and 8 weeks (week 49) after the last Env protein immunization. Bars represent medians. *$P \le 0.05$, **$P \le 0.01$, ***$P \le 0.001$, and ****$P \le 0.0001$ by 2-tailed Mann-Whitney.

Discussion

In the present study, we evaluated whether a vaccination strategy that stimulated robust cellular and antibody immune responses would confer enhanced protection against a mucosal challenge, relative to vaccines that induced either response alone. The data demonstrate that sequential immunization with 3 different viral vectors expressing Gag and a soluble Env protein adjuvanted with the synthetic TLR7/8 ligand 3M-052 in NP induced robust tissue-resident $CD8^+$ T cell and antibody responses and resulted in enhanced protection against a low-dose heterologous intravaginal challenge. In contrast immunization with HVV or Env + NP — which induced only $CD8^+$ T cells or Env-specific antibody responses, respectively — offered less protection. Following intravaginal challenges with the Tier 2 SHIV-1157ipd3N4, the reductions in per-exposure risk of infection were significantly higher after 10 challenges in younger animals vaccinated with the combined HVV, Env + NP regimen. Importantly, after 5 challenges, 80% of young and adolescent HVV, Env + NP–vaccinated animals were protected.

We demonstrated that the 3 intravenous HVV immunizations were able to generate a high magnitude of Gag-specific $CD4^+$ and $CD8^+$ T cells. Comparison of peak viral loads between vaccination groups and control animals showed significantly lower viral loads in animals that received HVV immunizations, indicating that the cellular responses efficiently controlled virus replication, as shown in other studies (35). In our study, analysis of polyfunctional T cells showed that double IFN-γ^+IL-2^+ or single IFN-γ^+CD8^+

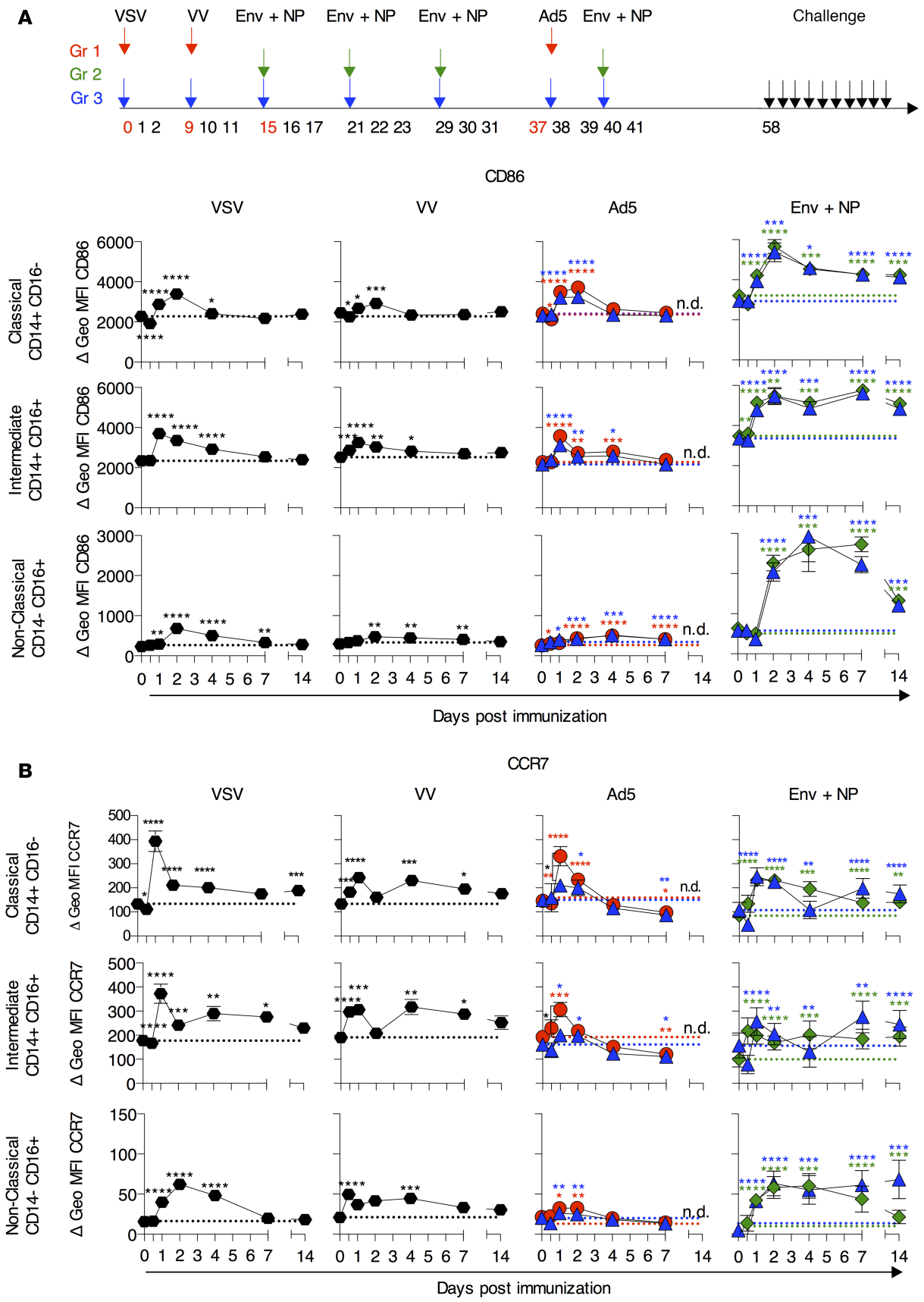
A
VSV
VV
Env + NP
Env + NP
Env + NP
Ad5
Env + NP
Challenge
Gr 1
Gr 2
Gr 3
0 1 2
9 10 11
15 16 17
21 22 23
29 30 31
37 38 39 40 41
58
CD86
VSV
VV
Ad5
Env + NP
Classical CD14+ CD16-
Intermediate CD14+ CD16+
Non-Classical CD14- CD16+
Δ Geo MFI CD86
n.d.
Days post immunization
B
CCR7
Δ Geo MFI CCR7
n.d.
Days post immunization

Figure 5. Sustained activation of monocyte subsets following Env + NP immunization. (**A**) Study overview. Activated ($CD86^+$) $CD14^+CD16^-$, $CD14^+CD16^+$, and $CD14^-CD16^+$ monocytes in blood after vaccination with viral vectors or Env protein. (**B**) Appearance of blood monocytes expressing the CCR7 chemokine receptor for homing to lymphoid organs after vaccination. Data represents the mean and ± SEM of the geometric mean difference (Δ) between isotype control and antibody staining values. Within each group, significant increases in cell levels relative to baseline were found using the Wilcoxon matched-pairs signed rank test. $^*P \le 0.05$, $^{**}P \le 0.01$, $^{***}P \le 0.001$, and $^{****}P \le 0.0001$. Statistical differences between vaccine groups were analyzed using the Mann-Whitney test and are indicated by a square bracket.

T cell subsets were associated with a lower viral load at the peak of infection. Although expression of Class I allele Mamu-A*01 is associated with a protective effect against disease progression (36, 37), we did not observe a significant difference between the peak viral loads or protection in Mamu-$A*01^+$ animals, excluding a major impact of this haplotype on the challenge outcome.

The effector functions and tissue localization of memory T cells are thought to be critical for protective immunity (38). We observed that heterologous prime boost vaccination with replicating vectors was capable of inducing memory $CD8^+$ T cells that localized within nonlymphoid tissues, including the reproductive mucosa, the site of viral challenge. In addition, the NP-encapsulated 3M-052 adjuvant used with soluble gp140 Env generated high-magnitude and durable Env-specific IgG antibodies both in serum and vaginal secretions. Robust plasmablast responses in the blood, as well as long-lived plasma cells in the BM, were also induced. Furthermore, the adjuvanted Env protein induced high titers of Tier 1A and Tier 1B neutralizing antibodies. Although it failed to induce neutralizing antibodies to the Tier 2 SHIV-1157ipd3N4 challenge virus, ADCVI results indicated that the Env immunogen did generate nonneutralizing serum antibodies that could mediate killing of SHIV-1157ipd3N4–infected cells in the presence of FcγR-expressing monocytes and NK cells.

The innate immune response, particularly activation of DCs via pathogen recognition receptors (PRRs), is known to play a key role in orchestrating the adaptive immune response to vaccination (39–43). We demonstrated in this study that NP-encapsulated 3M-052 induced a markedly pronounced and sustained activation of monocyte subsets as compared with other vector immunizations. Notably, enhanced expression of the costimulatory molecule CD86 on monocytes was observed as long as 2 weeks after vaccination. Recently, Vaccari et al. demonstrated that inflammasome activation in $CD14^+CD16^-$ monocytes following vaccination was associated with a reduced risk of SIV_{mac251} acquisition (44). Interestingly, we also found a significant direct correlation between classical $CD14^+CD16^-$ monocytes induced after the first Env + NP vaccination and delayed infection (data not shown). In contrast, there was inverse correlation between intermediate monocytes and protection in animals vaccinated with an Env + NP component (data not shown).

Importantly, we noticed an impact of age on the ability of vaccination to induce protective immunity. Enhanced protection was observed in young and adolescent (<8 years old) compared with older animals (>8 years old) vaccinated with HVV, Env + NP. Age-associated changes in innate and adaptive immune responses are well characterized and have been associated with reduced vaccine efficacy (45). Limited antibody responses in the elderly have been reported to be related to qualitative changes in antibody specificity, isotype, and affinity (46, 47). Here, aging was found to primarily affect the magnitude and persistence of serum binding antibodies. Young and adolescent animals developed higher levels of Env-specific serum IgG. In contrast, the magnitude of $CD4^+$ and $CD8^+$ T cell responses did not differ in young and old HVV-vaccinated animals, but we did notice a shift of the peripheral T cell pool from naive to central memory in the older animals (data not shown). Loss of naive T cells is associated with a loss of TCR repertoire diversity (48), and even though we did not demonstrate functional differences in response to vaccination, it is likely that it contributed to the reduced protection in older animals. Importantly, we also observed higher frequencies of $CD4^+CCR5^+$ HIV target T cells in older animals (data not shown), and this also may have contributed to the higher infection rate in these animals.

Analysis of correlates of acquisition rate revealed that the prechallenge levels of Env-specific IgG antibodies in serum and vaginal secretions, as well as titers of Tier 1 neutralizing antibodies and ADCVI against the challenge virus, were significantly associated with delayed acquisition in animals vaccinated with the HVV, Env + NP regimen. Rate of infection was also correlated with levels of anti–C1 IgG antibodies, which have been shown capable of mediating ADCC (49). Interestingly, we did not observe these correlations in animals vaccinated with Env + NP alone, although we found similar levels of antibodies in both groups. The fact that similar antibody responses did not have the same impact in both groups argues for a potential synergy between the humoral and cellular arms of the immune system.

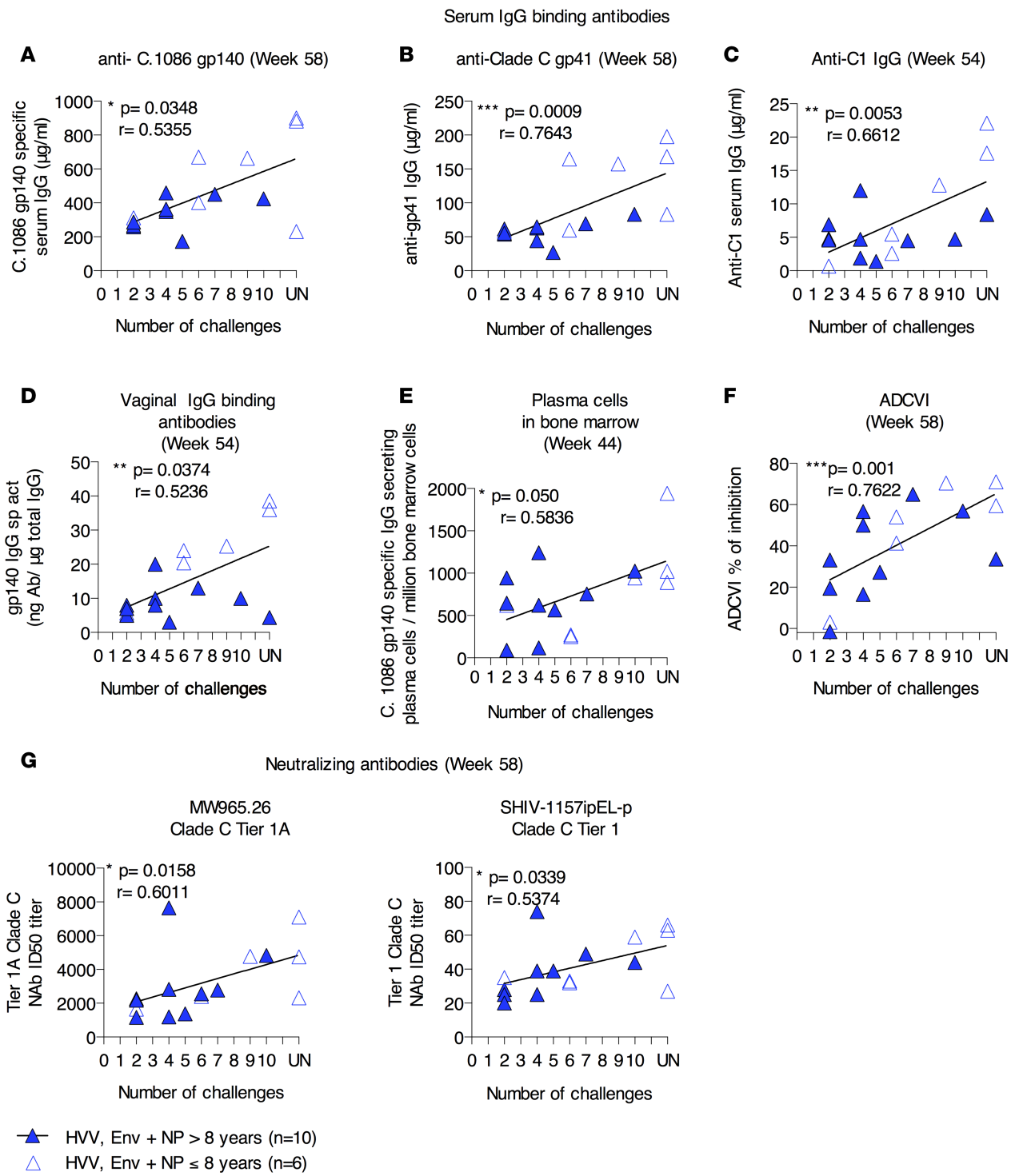

Figure 6. Associations between prechallenge antibody responses and rate of infection acquisition in HVV, Env + NP immunized animals. (A–G) Using the 2-tailed Spearman rank test, the rate of infection acquisition in HVV, Env + NP–vaccinated animals was found to be significantly correlated with concentrations of serum IgG antibodies against the gp140 immunogen, gp41 protein, and C1 peptide (**A–C**), levels of C.1086 gp140–specific vaginal IgG antibodies (**D**), numbers of anti–gp140 IgG– secreting plasma cells in BM (**E**), ADCVI activity against SHIV-1157ipd3N4 in serum (**F**), and titers of serum-neutralizing antibodies to Tier 1 Clade C viruses MW965.26 and SHIV-1157ipEL-p on the weeks indicated (**G**). In all graphs, open and closed triangles denote animals <8 and >8 years old, respectively. Correlation tests were performed using results for all animals in the HVV, Env + NP vaccination group.

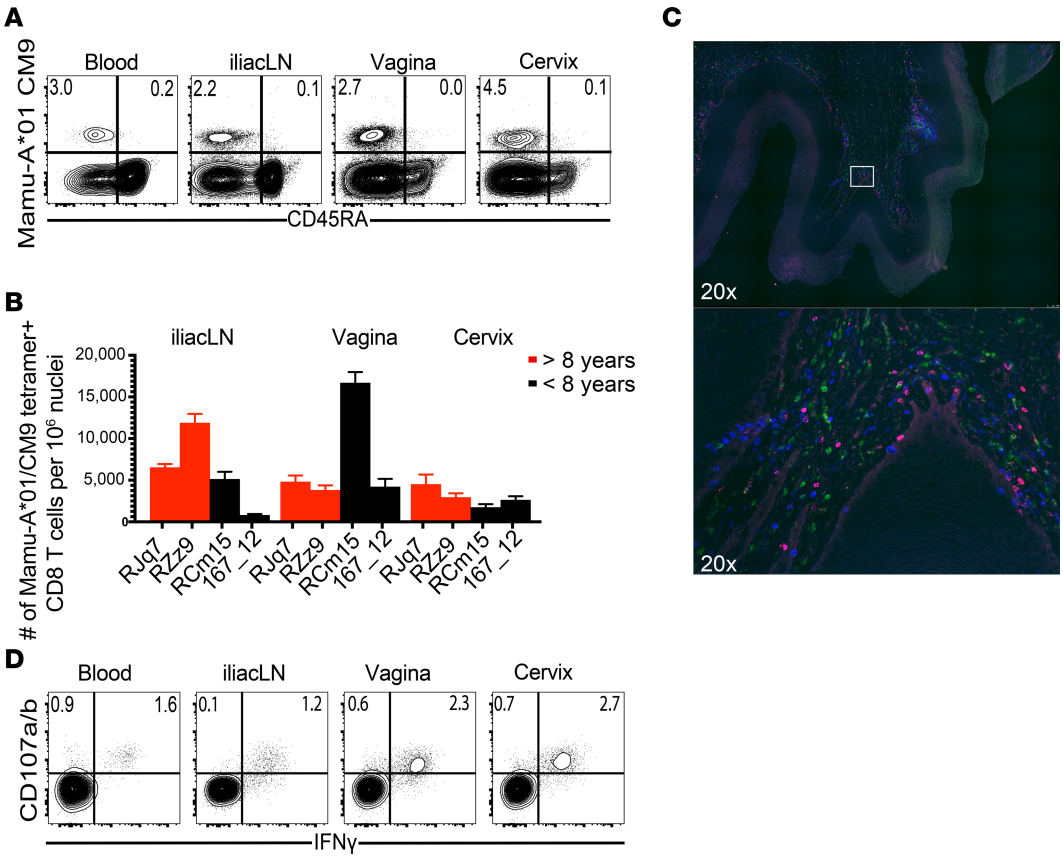

Figure 7. Distribution of SIV-specific CD8⁺ T cells in blood, iliac lymph node, vagina, and cervix. Representative dot plots illustrating frequencies of CM9 tetramer⁺CD8⁺ T cells in blood, iliac lymph node, vagina, and cervix of an HVV-vaccinated animal. (**B**) Numbers of CM9 tetramer⁺CD8⁺ T cells in iliac lymph node, vagina, and cervix of 2 HVV- and 2 HVV, Env + NP–vaccinated animals at necropsy (week 54). Results represent the mean ± SD determined after imaging multiple regions within sectioned tissue. (**C**) Confocal microscopy of vaginal tissue at week 54 (top) and zoomed-in area (bottom). Blue, CD8; red, tetramer; green, CD4. (**D**) Representative dot plots showing frequencies of memory CD8⁺ T cells expressing the CD107a/b degranulation marker and IFN-γ after CM9 peptide stimulation of lymphocytes isolated from blood, iliac lymph node, vagina, and cervix.

The precise mechanism by which such a synergy could operate remains to be elucidated. Numerous studies have shown that resident memory T cells accelerate pathogen control at barrier sites of infection, in the absence of humoral immunity. Potential synergy between TRM and humoral immunity has not been tested. It could be possible that humoral immunity alone is suboptimal in preventing infection of relevant founder populations, whereas TRM immunity alone is suboptimal at eliminating founder cells. Thus, antibodies and TRMs may synergize to offer enhanced protection, each operating through separate and unrelated mechanisms. In this context, it has been shown that, in response to antigen recognition in the reproductive mucosa, tissue-resident memory CD8⁺ T cells induce local chemokine expression and upregulation of VCAM-1 on vascular endothelium. This process is dependent on TRM-intrinsic expression of IFN-γ and is known to result in the rapid recruitment of α4β1⁺ B cells to the mucosae (33, 34). It is possible that TRM-derived IFN-γ provides a mechanism by which CD8⁺ T cell immunity might collaborate directly with the humoral immune system by amplifying the effects of local antibodies. Importantly, it remains to be investigated whether TRM might recruit plasma cells or augment local antibody concentrations through other mechanisms (e.g., by promoting transudation). Furthermore, TRMs are known to produce factors such as XCL1/lymphotactin, which has been shown to inhibit HIV at an early stage of infection, via blockade of viral attachment and entry into host cells (50). Recently, 2 important studies highlighted the notion of clearing the phase of initial viral dissemination by neutralizing antibodies with the demonstration that administrated HIV-neutralizing monoclonal antibodies can afford protection against SHIV infection (51) and clear infected foci in tissues (52).

These reports indicate that neutralizing antibodies, when present by passive immunization, are being recognized as capable of playing a role in sterile protection and postinfection control of SHIV infection. Hence, designing a vaccine that induces HIV-specific neutralizing antibodies concomitantly with the induction of T cell responses may delineate potent protection.

In conclusion, our results demonstrate the advantage of vaccines that induce combined $CD8^+$ T cell and antibody responses in offering enhanced protection against mucosal challenge. We demonstrate that the potentially novel adjuvant 3M-052 can induce a high magnitude and persistent antibody responses in mucosal and systemic compartments. Better definition of the functional properties of antibodies that contributed to protection, in addition to the use of trimeric Env immunogens that better induce Tier 2 neutralizing antibodies, should improve the efficacy of this promising heterologous prime boost vaccine strategy.

Methods

Animals, immunizations, and challenge

Eighty-one female RMs (*Macaca mulatta*), ages 3–16 years, were assigned to the study. Animals were confirmed negative for SIV and simian T cell lymphotropic virus (STLV) and were tested for the expression of Mamu-A*01, -B*08, and -B*17 alleles. TRIM5α genotyping was conducted as previously described (53). Animals were assigned to one of the immunization groups shown in Figure 1. Twenty-three animals in Group 1 received the Gag protein (SIVmac239 origin) encoding VSV, VV, and Ad5 vectors in sequence. VSV-Gag vector was given i.v. at a dose of 5×10^7 PFU per animal at week 0. VV-Gag vector was given i.v. at a dose of 1×10^7 PFU per animal at week 9 prior to i.v. boosting with Ad5-Gag at a dose of 7×10^{10} PFU per animal at week 37. Twenty-two animals in Group 2 received 100 μg of the HIV-1 Clade C gp140 C.1086 K160N envelope protein adjuvanted with 2.0 mg of PLGA NPs containing 75 μg of TLR7/8 agonist (3M-052). Twenty-one animals in Group 3 were immunized with viral vectors as in Group 1, along with the gp140 immunogen + NP adjuvant as in Group 2. Because of clinical issues, 1 animal from Group 1 was removed from the study. Four animals in each group were sacrificed 4 weeks before challenge in order to evaluate the prechallenge immune responses in tissues. Fifteen unvaccinated macaques were used as controls for the challenge experiment. RMs were challenged 10 times intravaginally with the SHIV-1157ipd3N4 virus expressing a heterologous Clade C envelope (22). The virus stock (8×10^6 $TCID_{50}$/ml) was used at a dilution of 1:21 and delivered in a volume of 1 ml of PBS (GE Healthcare Life Sciences). Plasma viral loads were measured weekly, and animals were considered infected after detection of >60 copy equivalents of SIV RNA per ml on 2 consecutive weeks. Once an animal was infected, further challenges were stopped.

Immunogens

Viral vectors expressing SIV Gag protein. Recombinant VSV serotype New Jersey (VSV-NJ) and recombinant VV (WR strain), each expressing full-length SIVmac239 Gag (54, 55), were generated as previously described (56–58). The immunizations with HVV were done by i.v. injecting 1 ml of recombinant VSV-Gag (rVSV-Gag) (59, 60), rVV-Gag, or rAd5-Gag (61) in the doses described above.

Recombinant Env protein. The recombinant trimeric gp140 C.1086 K160N Env protein was provided by Barton Haynes (Duke Human Vaccine Institute). This soluble Env gp140 protein was originally derived from an individual acutely infected with Clade C HIV-1. The cleavage site between gp120 and gp41 was mutated, and the lysine at position 160 was changed to asparagine. The protein was produced in 293F cells by transient transfection, purified using lectin chromatography, and filtered as described (62).

Synthesis of 3M-052 encapsulated PLGA NPs. The 3M-052 molecule was provided by 3M Drug Delivery Systems. Resomer RG502H, PLGA (Mw ~12,000) polymer was procured from Boehringer Ingelheim (now supplied by Evonik Industries). Poly(vinyl alcohol) (PVA; Mw 31,000-50,000) was purchased from MilliporeSigma. 3M-052–encapsulated PLGA NP formulations were synthesized using an oil in water (O/W) single emulsion followed by solvent evaporation process, as previously described, with slight modifications (9). PLGA polymer (200 mg) and 8.0 mg of 3M-052 were each solubilized in 1.0 ml of dichloromethane in 4.0 ml glass vials, followed by mixing. The oil phase containing PLGA and 3M-052 was added to 15 ml of a sterile filtered 5% PVA solution in 20.0 ml glass vials, followed by homogenization for 2.0 minutes using a speed setting of 6 with a Powergen Homogenizer (Thermo Fisher Scientific) at room temperature. This O/W emulsion was immediately added to 85.0 ml of the 5% PVA solution under magnetic stirring in 250 ml glass beakers to

allow solvent evaporation for 4 hours at room temperature. NPs formed were collected by centrifugation at 10,000 *g* for 30 minutes and washed twice using 0.2 μm sterile filtered deionized water. NPs were flash frozen in liquid nitrogen and lyophilized using a Freezone 2.5L benchtop lyophilizer (Labconco). All glassware used in the synthesis of particles were autoclaved, and solutions sterile filtered. NPs were verified for size distribution using a dynamic light scattering–based (DLS-based) particle sizer (Brookhaven Instruments). Encapsulation efficiency of 3M-052 was estimated using a UV-VIS scan, with peak noted at 327 nm as described before (9), and a standard curve established with known amounts of 3M-052.

Plasma viral load quantification

SIV RNA copy number was determined using quantitative PCR with sensitivities of 60 copies/ml. The assay was performed as described (63). All samples were run in duplicate, and the mean value is reported.

ICS

PBMC were isolated, and 2×10^6 cells were incubated in 200 μl of complete media (RPMI 1640 containing L-glutamine [Corning Life Sciences], 10% FBS [Corning Life Sciences], 10 mM HEPES [Lonza], 1× MEM nonessential amino acid [Corning Life Sciences], 1 mM sodium pyruvate [Lonza], 1 mM penicillin/streptomycin [Corning Life Sciences], and 1× 2-Mercaptoethanol [Thermo Fisher Scientific]) with anti-CD28 (1 μg/ml, CD28.2), anti-CD49d (1μg/ml, 9F10) (both BD Biosciences) and different conditions for stimulation as follows: (a) DMSO solvent for negative control; (b) Gag peptide pool (1–125 peptides derived from SIVmac239) at a concentration of 2 μg/ml; (c) $Gag_{181–189}$ CM9 peptide at a concentration of 1 μg/ml; (d) Envelope peptide pool 1 (peptide sequence 1–110) at a concentration of 2 μg/ml; (e) Env peptide pool 2 (peptide sequence 111–212) at a concentration of 2 μg/ml); and (f) PMA/Ionomycin for positive control. APC anti-human CXCR5 (clone MU5UBEE, e-Bioscience) and BV650 anti-human CD107a (clone H4A3, BioLegend) antibodies were added in culture before incubation. Brefeldin A (10 μg/ml, MilliporeSigma) was added after 2 hours of incubation, and cells were incubated for an additional 4 hours. Cells were transferred to 4°C overnight and stained the next day for expression of cytokines. After washing, dead cells were stained in PBS for 30 minutes with APC-Cy7 Viability dye. After washing in staining buffer (PBS containing 5% FBS), cells were stained with surface antibodies for 30 minutes with the following markers: PerCP anti–human CD8 (clone RPA-T8, BioLegend), BV605 anti–human CD4 (clone 3A3N-2.1, BioLegend), and BV786 anti–human CCR5 (clone 3A9, BD Biosciences). After 2 washes in staining buffer, cells were fixed and permeabilized with CytoFix/Cytoperm buffer (BD Bioscience) for 10 minutes. Cells were washed 2 times with BD PermWash buffer and then stained for 30 minutes in PermWash for intracellular cytokines using the following antibodies: FITC anti–human IL-2 (clone MQ1-17H12, BioLegend), PE anti–human IL-4 (clone 8D4-8, BioLegend), PE-Texas Red anti–human CD3 (clone SP34-2, BD Biosciences), PE-Cy7 anti–human TNF-α (clone Mab11, eBioscience), BV421 anti–human IL-21 (clone 3A3N-2.1, BD Biosciences), BV711 anti–human CD40L (clone 24-31, BioLegend), and A700 anti–human IFN-γ (clone 4S.B3, BioLegend). Cells were washed 2 times with PermWash and 1 time with staining buffer before being resuspended in 200 μl of wash buffer and acquired with the BD LSR II Flow Cytometer (BD Biosciences). Flow cytometry data were analyzed using Flowjo software (TreeStar Inc.).

Tetramer staining

MHC Class I tetramers were prepared and conjugated to streptavidin APC fluorophore as described (64). Frequencies of SIV-specific $CD8^+$ T cells were assessed using soluble tetrameric Mamu-A*01 MHC Class I tetramers specific for SIVmac239 immunodominant peptide $Gag_{181–189}$ CM9 (CTPYDINQM). Briefly, after isolation of lymphocytes from blood, cells were stained with CM9-APC tetramer, along with the following surface antibodies: PerCP anti–human CD4 (clone OKT4, BioLegend), PE-Texas Red anti–human CD28 (clone CD28.2, BioLegend), PE-Cy7 anti–human CD127 (clone eBioRDR5, eBioscience), Pac Blue anti–human CCR7 (clone G043H7, BioLegend), BV510 anti–human CXCR3 (clone G025H7, BioLegend), BV605 anti–human CD95 (clone DX2, BioLegend), BV655 anti–human CD45Ra (clone MEM-56, Invitrogen), BV711 anti–human CD8a (clone RPA-T8, BioLegend), and A700 anti–human CD3 (clone SP-34-2, BD Biosciences). Cells were then fixed and permeabilized using the Fix/Perm and Perm/Wash buffer (BD Biosciences) before intracellular staining with FITC anti–human Ki67 (clone B56, BD Biosciences) and PE anti–human Granzyme B (clone GB12, Invitrogen). Tetramer frequencies and phenotypic markers were assessed using a BD LSR Fortessa flow cytometer (BD Biosciences), and data were analyzed using Flowjo software.

Innate cell staining

PBMC were isolated from blood, and 2 × 10^6 cells were used for staining. After washing in PBS, cells were stained 30 minutes for dead cells with Efluor 506 Viability dye (eBioscience). Cells were washed and stained with anti–human CADM1 antibody (chicken IgY, clone 3E1, MBL International) for 30 minutes. After 2 washes in staining buffer, cells were stained in 100 μl for surface markers using an antibody cocktail including: FITC anti–human DEC205 (clone MG38, eBioscience), PE anti–human BDCA-1 (clone AD5-8E7, Miltenyi Biotec), PerCP anti–chicken IgY $F(ab')_2$ (Jackson ImmunoResearch), PE-Cy7 anti–human CD123 (clone 7G3, BD Biosciences), PE-CF594 anti–human CD3 (clone SP34-2, BD Biosciences), BV421 anti–human CCR7 (clone G043H7, BioLegend), Qdot605 anti–human CD14 (clone TUk4 Invitrogen), BV650 anti–human CD86 (clone IT2.2, BioLegend), BV711 anti–human HLA-DR (clone L243, BioLegend), BV800 anti–human (clone RPA-T8, BioLegend), APC anti–human CD11c (clone S-HCL-3, BD Biosciences), A700 anti–human CD16 (clone 3G8, BioLegend), and APC-Cy7 anti–human CD20 (clone 2H7, BioLegend). Cells were washed 2 times with staining buffer and fixed with Cytofix (BD Biosciences) for 10 minutes. Finally, cells were washed 1 time with staining buffer and resuspended in 200 μl FACS buffer before being acquired on BD LSR Fortessa flow cytometer. Flow cytometry data were analyzed using Flowjo software.

Binding antibodies

ELISA was used as described (10) to measure serum binding antibodies to the gp140 C.1086 K160N Env protein immunogen, Clade C gp41 (Immune Technology), C1 peptide, SHIV-gp120 1157ipd3N4, and murine leukemia virus leukemia virus gp70 scaffolded SHIV-1157ipd3N4 V1V2 loops (both from Abraham Pinter, Rutgers Medical School, Newark, New Jersey, USA). Briefly, plates coated with 100 ng protein per well, blocked, and loaded with serial dilutions of standard and test sera. The standard were IgG-depleted serum (for IgM assays) or IgA or IgG purified, respectively, with Peptide M agarose (Invitrogen) or Protein G sepharose (GE Healthcare) from pooled serum of SHIV-infected macaques that received Clade C vaccines in previous studies (24). The antibody concentrations in the standards were estimated as described (65). Plates were developed with tetramethylbenzidine substrate (SouthernBiotech) after treatment with peroxidase-labeled goat anti–monkey IgG (AlphaDiagnostics, catalog 70021) or biotinylated goat anti–monkey IgG (catalog 617-406-002), –monkey IgA (catalog 617-106-006), or –human IgM antibodies (catalog 609-107) (all from Rockland) followed by neutralite avidin-peroxidase (SouthernBiotech). For all IgA assays, samples were first depleted of IgG using Protein G sepharose (GE Healthcare) as described (66) due to cross-reactivity of the anti–monkey IgA secondary antibody with macaque IgG. A binding antibody multiplex assay (BAMA) was used as described (67) with the standards above to measure vaginal antibodies to C.1086 gp140 and serum antibodies to peptides representing the consensus C gp120 constant domain 1 (C1; MHEDIISLWDESLKPCVKLTPLCV; Neolabs), V3 loop (cysteine-bonded CTRPNNNTRKSIRIGPGQTFYATGDIIGDIRQAHC; Neolabs), and the C.1086 gp41 immunodominant region (DQQLLGMWGCSGKLIC with cysteines bonded; Genscript). Peptides were synthesized with KKK at the N-terminus to improve solubility. Pur-A-lyzer Midi 1000 tubes (MilliporeSigma) were used to dialyze peptides in PBS prior to conjugation to BioPlex-Pro magnetic carboxylated beads (Bio-Rad). Serial dilutions of serum or vaginal secretions eluted from Weck-Cel sponges (10) were reacted with beads overnight at 1100 rpm and 4°C. Fluorescence was recorded in a Bio-Rad Bioplex 200 after development with above biotinylated antibodies and 1/400 neutralite avidin-phycoerythrin (SouthernBiotech). For vaginal secretions, the concentrations of antigen-specific IgA and IgG interpolated from standard curves were adjusted relative to the total IgA and IgG concentrations to determine the specific activity (ng IgA or IgG antibodies per μg of total IgA or IgG). Total IgA and IgG were measured by ELISA, as described (66), using goat anti–monkey IgA or IgG (AlphaDiagnostics) capture antibodies, a calibrated rhesus reference serum (from Michael Russell, University at Buffalo, Buffalo, New York, USA), and the above biotinylated secondary antibodies.

Ab avidity

The avidity of serum IgG Abs to gp140 C.1086 or gp120 1157ipd3N4 protein was measured using NaSCN displacement ELISA as described (67). The avidity index was calculated by dividing the concentration of antibodies in wells treated with 1.5 M NaSCN for 10 minutes at 37°C by the concentration of antibodies in untreated wells.

ADCVI

Assays for ADCVI activity in serum were done as previously described (68), with the exception that target cells were infected by spinoculation and the effector cells were cryopreserved human PBMC. Briefly, on day 1, $CCR5^+$ CEM-NKR cells (a gift from Jim Hoxie, University of Pennsylvania, Philadelphia, Pennsylvania, USA) were centrifuged with SHIV-1157ipd3N4 and 15 μg/ml polybrene at 1200 *g* for 90 minutes and then cultured for 2 days in the presence of 10 ng/ml TNF-α and polybrene. On day 2, cryopreserved PBMC were washed, added to wells of a V-bottom plate in 100 μl of medium containing 1×10^5 cells, and allowed to rest for 24 hours at 37°C in 5% CO_2. On day 3, 50 μl of 1/25 sterile-filtered serum and 50 μl containing 1×10^4 washed, infected CEM-NKR cells were added to wells. On day 7, the cells were washed twice to remove Gag Ab. On day 10, the culture medium was harvested and the viral content was measured by p27 ELISA as described (68).

Virus neutralization assays

Neutralizing antibody activity was measured in 96-well culture plates by using Tat-regulated luciferase (Luc) reporter gene expression to quantify reductions in virus infection in TZM-bl cells. TZM-bl cells were obtained from the NIH AIDS Research and Reference Reagent Program. Assays were performed as described previously (69) using HIV-1 Env–pseudotyped viruses (MW965.26 and 6644.v2.c33) produced in 293T cells or replication competent viruses (SHIV-1157ipd3N4) grown in activated human PBMCs. Test samples were diluted over a range of 1:20–1:43,740 in cell culture medium and preincubated with virus (~150,000 relative light unit equivalents) for 1 hour at 37°C before addition of cells. Following a 48-hour incubation, cells were lysed and Luc activity determined using a microtiter plate luminometer and BriteLite Plus Reagent (Perkin Elmer). Neutralization titers are the sample dilution (for serum) or antibody concentration (for soluble CD4 [sCD4], purified IgG preparations, and monoclonal antibodies) at which relative luminescence units (RLU) were reduced by 50% compared with RLU in virus control wells after subtraction of background RLU in cell control wells. Serum samples were heat-inactivated at 56oC for 1 hr prior to assay.

Plasmablasts and plasma cells

ELISPOT assays were performed as previously described (70). Briefly, 96-well multiscreen HTS filter plates (MilliporeSigma, MSHAN4B50) were coated overnight at 4°C with 10 μg/ml of anti–monkey IgG, –IgA, or –IgM (H&L) goat antibody (Rockland) or with 2 μg/ml of recombinant HIV gp140 or SIV Gag protein (Immune Technology Corp.) for enumeration of total or antigen-specific antibody-secreting cells (ASCs), respectively. Wells were washed 4 times with PBS containing 0.05% Tween 20 (PBS-T) and 4 times with PBS, and they were blocked with complete RPMI medium for 2 hours in a 5% CO_2 incubator at 37°C. Whole PBMC preparations were diluted in complete RPMI medium, plated in serial 3-fold dilutions, and incubated overnight in a 5% CO_2 incubator at 37°C. Wells were washed 4 times with PBS and 4 times with PBS-T, followed by incubation for 2 hours at room temperature with either anti–monkey IgG-, IgA-, or IgM-biotin conjugated antibodies (Rockland) diluted 1:1000 in PBS-T with 1% FBS solution (PBS-T-F). Wells were again washed 4 times with PBS-T before adding Avidin D-HRP (Vector Laboratories) diluted 1:1000 in PBS-T-F. After a 3-hour incubation at room temperature, wells were washed 4 times with PBS-T and 4 times with PBS. Spots were developed with filtered 3-amino 9-ethylcarbazole (AEC) substrate (0.3 mg/ml AEC diluted in 0.1 M of sodium acetate buffer [pH 5.0], containing a 1:1000 dilution of 3% hydrogen peroxide). To stop the reaction, wells were washed with water. Spots were documented and counted using the Immunospot CTL counter and Image Acquisition 4.5 software (Cellular Technology). Once counted, the number of spots specific for each immunoglobulin isotype was reported as the number of either total or antigen-specific ASCs per million PBMCs.

In situ tetramer staining and immunofluorescence microscopy

Two hundred to 400 μm transverse tissue sections were made from fresh tissue using a surgical blade. Tissue sections were incubated with MHC Class I tetramers conjugated to streptavidin PE fluorophore (MilliporeSigma) overnight in PBS containing 2% heat-inactivated FBS and 2% normal goat serum (Thermo Fisher Scientific). Sections were washed with PBS, fixed with 2% paraformaldehyde for 2 hours, washed, and sucrose embedded for 16 hours. Tissue was then snap frozen in OCT (Sakura) and prepared as

described previously (71). Frozen sections were fixed in acetone and stained using AF647 antihuman CD4 (clone OKT4, BioLegend), AF488 antihuman CD8α (clone SK1, BioLegend), and DAPI to distinguish nucleated cells. Immunofluorescence microscopy was performed as in Schenkel et al. (72). Cells were considered tetramer positive by coexpression of CD8α, tetramer, and DAPI and negativity for CD4.

Statistics

Kaplan Meier curves were used to depict acquisition of infection in animals after viral challenge. Mantel Cox Log-rank test and Gehan-Breslow test were used to infer statistical significance between survival curves between the vaccinated groups vs. unvaccinated controls. The 2-tailed Mann-Whitney rank sum test was used to compare immune responses between 2 different immunization or age groups. Multigroup comparisons for all immunological readouts were performed using the Kruskal-Wallis test followed by Dunn's correction. The Wilcoxon matched-pairs signed rank test was used to compare changes in frequencies of innate cells compared with baseline. Two-tailed Spearman rank correlation test was used for correlations. Statistical analyses were performed using GraphPad Prism software version 6.

Study approval

The present study was reviewed and approved by the Emory University IACUC guidelines located at Emory University.

Author contributions

BP, D. Masopust, EH, RRA, SPK, FV, and DB designed the research. CP, SPK, PAK, RN, CQ, PBJR, LMS, PP, TL, YOK, and CCL conducted experiments. CP, SPK, PAK, RN, CQ, PBJR, CAD, LMS, PP, TL, YOK, CCL, D. Montefiori, and JW analyzed the data. MT, JV, BH, CYK, JSG, and JWY provided key reagents. CP, BP, PAK, and D. Masopust wrote the manuscript.

Acknowledgments

We thank all animal staff at the Yerkes National Primate Research Center and Emory University for help with the macaque study, Lydia Benitez and Brenda Wehrle for technical assistance in processing samples and performing staining, Robert Wilson and Korey Walter for processing secretions and performing ELISAs, and the CFAR Immunology/Emory Vaccine Center Flow cytometry core. This work was supported by NIH grants UM1 AI124436 (Consortia for AIDS Vaccine Research in Non-Human Primates) and NIAID UM1AI100663 (Center for HIV/AIDS Vaccine Immunology and Immunogen Discovery). We acknowledge the NIH AIDS Reagent Program for Gag and Env peptide pool reagents.

Address correspondence to: Bali Pulendran, 279 Campus Drive, Beckman Center B225A, Stanford University, Stanford, California 94305, USA. Phone: 404.309.9126; Email: bpulend@stanford.edu. Or to: David Masopust, 2-182 MBB 2101 6th SE, Minneapolis, Minnesota 55455, USA. Phone: 612.625.5869; Email: masopust@umn.edu.

CP's present address is: Unité Physiologie et Pathologie Moléculaires des Rétrovirus Endogènes et Infectieux, CNRS UMR9196, Gustave Roussy, Villejuif F-94805, France.

1. Burton DR, Hangartner L. Broadly Neutralizing Antibodies to HIV and Their Role in Vaccine Design. *Annu Rev Immunol*. 2016;34:635–659.
2. de Taeye SW, Moore JP, Sanders RW. HIV-1 Envelope Trimer Design and Immunization Strategies To Induce Broadly Neutralizing Antibodies. *Trends Immunol*. 2016;37(3):221–232.
3. Rerks-Ngarm S, et al. Vaccination with ALVAC and AIDSVAX to prevent HIV-1 infection in Thailand. *N Engl J Med*. 2009;361(23):2209–2220.
4. Haynes BF, et al. Immune-correlates analysis of an HIV-1 vaccine efficacy trial. *N Engl J Med*. 2012;366(14):1275–1286.
5. Pulendran B, Ahmed R. Immunological mechanisms of vaccination. *Nat Immunol*. 2011;12(6):509–517.
6. Coffman RL, Sher A, Seder RA. Vaccine adjuvants: putting innate immunity to work. *Immunity*. 2010;33(4):492–503.
7. Querec T, et al. Yellow fever vaccine YF-17D activates multiple dendritic cell subsets via TLR2, 7, 8, and 9 to stimulate polyvalent immunity. *J Exp Med*. 2006;203(2):413–424.
8. Querec TD, et al. Systems biology approach predicts immunogenicity of the yellow fever vaccine in humans. *Nat Immunol*. 2009;10(1):116–125.
9. Kasturi SP, et al. Programming the magnitude and persistence of antibody responses with innate immunity. *Nature*.

2011;470(7335):543–547.
10. Kasturi SP, et al. Adjuvanting a Simian Immunodeficiency Virus Vaccine with Toll-Like Receptor Ligands Encapsulated in Nanoparticles Induces Persistent Antibody Responses and Enhanced Protection in TRIM5α Restrictive Macaques. *J Virol*. 2017;91(4):e01844-16.
11. McMichael AJ. Is a Human CD8 T-Cell Vaccine Possible, and if So, What Would It Take? Could a CD8+ T-Cell Vaccine Prevent Persistent HIV Infection? *Cold Spring Harb Perspect Biol*. 2018;10(9):a029124.
12. Hansen SG, et al. Profound early control of highly pathogenic SIV by an effector memory T-cell vaccine. *Nature*. 2011;473(7348):523–527.
13. Jones RB, Walker BD. HIV-specific $CD8^+$ T cells and HIV eradication. *J Clin Invest*. 2016;126(2):455–463.
14. Akondy RS, et al. Initial viral load determines the magnitude of the human CD8 T cell response to yellow fever vaccination. *Proc Natl Acad Sci USA*. 2015;112(10):3050–3055.
15. Miller JD, et al. Human effector and memory CD8+ T cell responses to smallpox and yellow fever vaccines. *Immunity*. 2008;28(5):710–722.
16. Masopust D, Ha SJ, Vezys V, Ahmed R. Stimulation history dictates memory CD8 T cell phenotype: implications for prime-boost vaccination. *J Immunol*. 2006;177(2):831–839.
17. Vezys V, et al. Memory CD8 T-cell compartment grows in size with immunological experience. *Nature*. 2009;457(7226):196–199.
18. Fraser KA, Schenkel JM, Jameson SC, Vezys V, Masopust D. Preexisting high frequencies of memory CD8+ T cells favor rapid memory differentiation and preservation of proliferative potential upon boosting. *Immunity*. 2013;39(1):171–183.
19. Smirnov D, Schmidt JJ, Capecchi JT, Wightman PD. Vaccine adjuvant activity of 3M-052: an imidazoquinoline designed for local activity without systemic cytokine induction. *Vaccine*. 2011;29(33):5434–5442.
20. Fox CB, et al. Adsorption of a synthetic TLR7/8 ligand to aluminum oxyhydroxide for enhanced vaccine adjuvant activity: A formulation approach. *J Control Release*. 2016;244(Pt A):98–107.
21. Bercovitch FB, et al. A longitudinal study of age-specific reproductive output and body condition among male rhesus macaques, Macaca mulatta. *Naturwissenschaften*. 2003;90(7):309–312.
22. Song RJ, et al. Molecularly cloned SHIV-1157ipd3N4: a highly replication- competent, mucosally transmissible R5 simian-human immunodeficiency virus encoding HIV clade C Env. *J Virol*. 2006;80(17):8729–8738.
23. Kwa S, et al. CD40L-adjuvanted DNA/modified vaccinia virus Ankara simian immunodeficiency virus SIV239 vaccine enhances SIV-specific humoral and cellular immunity and improves protection against a heterologous SIVE660 mucosal challenge. *J Virol*. 2014;88(17):9579–9589.
24. Zhao J, et al. Preclinical studies of human immunodeficiency virus/AIDS vaccines: inverse correlation between avidity of anti-Env antibodies and peak postchallenge viremia. *J Virol*. 2009;83(9):4102–4111.
25. Hessell AJ, et al. Fc receptor but not complement binding is important in antibody protection against HIV. *Nature*. 2007;449(7158):101–104.
26. Xiao P, et al. Multiple vaccine-elicited nonneutralizing antienvelope antibody activities contribute to protective efficacy by reducing both acute and chronic viremia following simian/human immunodeficiency virus SHIV89.6P challenge in rhesus macaques. *J Virol*. 2010;84(14):7161–7173.
27. Chamcha V, et al. Strong, but Age-Dependent, Protection Elicited by a Deoxyribonucleic Acid/Modified Vaccinia Ankara Simian Immunodeficiency Virus Vaccine. *Open Forum Infect Dis*. 2016;3(1):ofw034.
28. Asquith M, et al. Age-dependent changes in innate immune phenotype and function in rhesus macaques (Macaca mulatta). *Pathobiol Aging Age Relat Dis*. 2012;2.
29. Pinti M, et al. Aging of the immune system: Focus on inflammation and vaccination. *Eur J Immunol*. 2016;46(10):2286–2301.
30. Blink EJ, Light A, Kallies A, Nutt SL, Hodgkin PD, Tarlinton DM. Early appearance of germinal center-derived memory B cells and plasma cells in blood after primary immunization. *J Exp Med*. 2005;201(4):545–554.
31. Blanchard-Rohner G, Pulickal AS, Jol-van der Zijde CM, Snape MD, Pollard AJ. Appearance of peripheral blood plasma cells and memory B cells in a primary and secondary immune response in humans. *Blood*. 2009;114(24):4998–5002.
32. Wrammert J, et al. Rapid cloning of high-affinity human monoclonal antibodies against influenza virus. *Nature*. 2008;453(7195):667–671.
33. Schenkel JM, Fraser KA, Beura LK, Pauken KE, Vezys V, Masopust D. T cell memory. Resident memory CD8 T cells trigger protective innate and adaptive immune responses. *Science*. 2014;346(6205):98–101.
34. Ariotti S, et al. T cell memory. Skin-resident memory $CD8^+$ T cells trigger a state of tissue-wide pathogen alert. *Science*. 2014;346(6205):101–105.
35. Janes H, et al. Vaccine-induced gag-specific T cells are associated with reduced viremia after HIV-1 infection. *J Infect Dis*. 2013;208(8):1231–1239.
36. Zhang ZQ, et al. Mamu-A*01 allele-mediated attenuation of disease progression in simian-human immunodeficiency virus infection. *J Virol*. 2002;76(24):12845–12854.
37. Mothé BR, et al. Expression of the major histocompatibility complex class I molecule Mamu-A*01 is associated with control of simian immunodeficiency virus SIVmac239 replication. *J Virol*. 2003;77(4):2736–2740.
38. Schenkel JM, Masopust D. Tissue-resident memory T cells. *Immunity*. 2014;41(6):886–897.
39. Pulendran B. The varieties of immunological experience: of pathogens, stress, and dendritic cells. *Annu Rev Immunol*. 2015;33:563–606.
40. Kastenmüller W, Kastenmüller K, Kurts C, Seder RA. Dendritic cell-targeted vaccines--hope or hype? *Nat Rev Immunol*. 2014;14(10):705–711.
41. Reed SG, Orr MT, Fox CB. Key roles of adjuvants in modern vaccines. *Nat Med*. 2013;19(12):1597–1608.
42. Pulendran B. Division of labor and cooperation between dendritic cells. *Nat Immunol*. 2006;7(7):699–700.
43. Thompson EA, Loré K. Non-human primates as a model for understanding the mechanism of action of toll-like receptor-based vaccine adjuvants. *Curr Opin Immunol*. 2017;47:1–7.
44. Vaccari M, et al. HIV vaccine candidate activation of hypoxia and the inflammasome in CD14+ monocytes is associated with a decreased risk of SIVmac251 acquisition. *Nat Med*. 2018;24(6):847–856.

45. Weinberger B, Herndler-Brandstetter D, Schwanninger A, Weiskopf D, Grubeck-Loebenstein B. Biology of immune responses to vaccines in elderly persons. *Clin Infect Dis*. 2008;46(7):1078–1084.
46. Weksler ME, Szabo P. The effect of age on the B-cell repertoire. *J Clin Immunol*. 2000;20(4):240–249.
47. Romero-Steiner S, et al. Reduction in functional antibody activity against Streptococcus pneumoniae in vaccinated elderly individuals highly correlates with decreased IgG antibody avidity. *Clin Infect Dis*. 1999;29(2):281–288.
48. Cicin-Sain L, et al. Loss of naive T cells and repertoire constriction predict poor response to vaccination in old primates. *J Immunol*. 2010;184(12):6739–6745.
49. Bonsignori M, et al. Antibody-dependent cellular cytotoxicity-mediating antibodies from an HIV-1 vaccine efficacy trial target multiple epitopes and preferentially use the VH1 gene family. *J Virol*. 2012;86(21):11521–11532.
50. Guzzo C, et al. The CD8-derived chemokine XCL1/lymphotactin is a conformation-dependent, broad-spectrum inhibitor of HIV-1. *PLoS Pathog*. 2013;9(12):e1003852.
51. Hessell AJ, et al. Early short-term treatment with neutralizing human monoclonal antibodies halts SHIV infection in infant macaques. *Nat Med*. 2016;22(4):362–368.
52. Liu J, et al. Antibody-mediated protection against SHIV challenge includes systemic clearance of distal virus. *Science*. 2016;353(6303):1045–1049.
53. Reynolds MR, et al. The TRIM5{alpha} genotype of rhesus macaques affects acquisition of simian immunodeficiency virus SIVsmE660 infection after repeated limiting-dose intrarectal challenge. *J Virol*. 2011;85(18):9637–9640.
54. Schwartz S, Campbell M, Nasioulas G, Harrison J, Felber BK, Pavlakis GN. Mutational inactivation of an inhibitory sequence in human immunodeficiency virus type 1 results in Rev-independent gag expression. *J Virol*. 1992;66(12):7176–7182.
55. Rosati M, et al. DNA vaccines expressing different forms of simian immunodeficiency virus antigens decrease viremia upon SIVmac251 challenge. *J Virol*. 2005;79(13):8480–8492.
56. Wu K, Kim GN, Kang CY. Expression and processing of human immunodeficiency virus type 1 gp160 using the vesicular stomatitis virus New Jersey serotype vector system. *J Gen Virol*. 2009;90(Pt 5):1135–1140.
57. An HY, Kim GN, Wu K, Kang CY. Genetically modified VSV(NJ) vector is capable of accommodating a large foreign gene insert and allows high level gene expression. *Virus Res*. 2013;171(1):168–177.
58. Bennink JR, Yewdell JW, Smith GL, Moller C, Moss B. Recombinant vaccinia virus primes and stimulates influenza haemagglutinin-specific cytotoxic T cells. *Nature*. 1984;311(5986):578–579.
59. Sacha JB, et al. Gag-specific CD8+ T lymphocytes recognize infected cells before AIDS-virus integration and viral protein expression. *J Immunol*. 2007;178(5):2746–2754.
60. Seder RA, et al. Protection against malaria by intravenous immunization with a nonreplicating sporozoite vaccine. *Science*. 2013;341(6152):1359–1365.
61. Quinn KM, et al. Comparative analysis of the magnitude, quality, phenotype, and protective capacity of simian immunodeficiency virus gag-specific CD8+ T cells following human-, simian-, and chimpanzee-derived recombinant adenoviral vector immunization. *J Immunol*. 2013;190(6):2720–2735.
62. Liao HX, et al. Antigenicity and immunogenicity of transmitted/founder, consensus, and chronic envelope glycoproteins of human immunodeficiency virus type 1. *J Virol*. 2013;87(8):4185–4201.
63. Amara RR, et al. Control of a mucosal challenge and prevention of AIDS by a multiprotein DNA/MVA vaccine. *Science*. 2001;292(5514):69–74.
64. Altman JD, et al. Phenotypic analysis of antigen-specific T lymphocytes. *Science*. 1996;274(5284):94–96.
65. Manrique M, et al. Long-term control of simian immunodeficiency virus mac251 viremia to undetectable levels in half of infected female rhesus macaques nasally vaccinated with simian immunodeficiency virus DNA/recombinant modified vaccinia virus Ankara. *J Immunol*. 2011;186(6):3581–3593.
66. Kozlowski PA, Lynch RM, Patterson RR, Cu-Uvin S, Flanigan TP, Neutra MR. Modified wick method using Weck-Cel sponges for collection of human rectal secretions and analysis of mucosal HIV antibody. *J Acquir Immune Defic Syndr*. 2000;24(4):297–309.
67. Nabi R, et al. Differences in serum IgA responses to HIV-1 gp41 in elite controllers compared to viral suppressors on highly active antiretroviral therapy. *PLoS ONE*. 2017;12(7):e0180245.
68. Kannanganat S, et al. High Doses of GM-CSF Inhibit Antibody Responses in Rectal Secretions and Diminish Modified Vaccinia Ankara/Simian Immunodeficiency Virus Vaccine Protection in TRIM5α-Restrictive Macaques. *J Immunol*. 2016;197(9):3586–3596.
69. Montefiori DC. Measuring HIV neutralization in a luciferase reporter gene assay. *Methods Mol Biol*. 2009;485:395–405.
70. Wrammert J, et al. Rapid cloning of high-affinity human monoclonal antibodies against influenza virus. *Nature*. 2008;453(7195):667–671.
71. Steinert EM, et al. Quantifying Memory CD8 T Cells Reveals Regionalization of Immunosurveillance. *Cell*. 2015;161(4):737–749.
72. Schenkel JM, Fraser KA, Vezys V, Masopust D. Sensing and alarm function of resident memory $CD8^+$ T cells. *Nat Immunol*. 2013;14(5):509–513.